XV International Conference on Computational Plasticity. Fundamentals and Applications
COMPLAS 2019
E. Oñate, D.R.J. Owen, D. Peric , M. Chiumenti, and Eduardo de Souza Neto (Eds)

HEAT TRANSPORT WITH ADVECTION IN FRACTURED ROCK

A. PÉREZ*, I.CAROL* AND P.PRAT*

* Department of Civil and Environmental Engineering
Universitat Politècnica de Catalunya (UPC)
Jordi Girona 1, D2 Building, E-08034 Barcelona, Spain
e-mail: adria.perez@upc.edu, ignacio.carol@upc.edu, pere.prat@upc.edu

Key words: Large advection, heat transport, zero-thickness interface elements, Péclet number, FEM, SUPG.

Abstract. In the transport of heat in porous media, diffusion generally dominates over advection due to slow fluid velocities imposed by low permeability. This is the reason why standard Galerkin formulation leading to extra non-symmetric matrix terms may be still used successfully. However, in the presence of fractures the situation may be different. Fractures constitute preferential flow paths where fluid velocities may be significant and advection may become dominant over diffusion ("large advection" with Péclet number >1). This paper focuses on the formulation, numerical implementation and verification of a model to solve the steady-state heat transport problem with large advection along geomechanical discontinuities represented by zero-thickness interface elements. The fluid velocity field is considered as known input data (no hydraulic coupling). The existing SUPG method is modified for its application to zero-thickness interface elements, and the resulting formulation is implemented in an existing FE geomechanical code. An example of application is presented with large advection along a discontinuity crossing a low permeability domain. The results show that the proposed approach leads to stable results, in contrast to standard Galerkin.

1 INTRODUCTION

The two main mechanisms of heat transport in saturated porous media are diffusion and advection. In the numerical formulation of the problem via the FEM, it is well known that, if advection dominates over diffusion (Péclet number $Pe > 1$), traditional Galerkin formulations cease to work [1]. In many practical engineering situations, however, such as in the case of geological materials, average fluid (Darcy) velocities may remain small due to the low permeability and tortuosity of the pore system, and this problem may be ignored.

But this situation may change in the presence of open fractures or cracks, because these may become preferential paths for fluid circulation with fluid velocities significantly higher than those found in the surrounding porous medium, and therefore exceeding the limit condition $Pe > 1$. Thus, it is important to establish a methodology to solve the large advection problem, especially for fractures or cracks.

1.1 Governing equations

The three-dimensional *transient heat conduction-advection differential equation* may be written as follows [1]:

$$\rho c \left(\frac{\partial \phi}{\partial t} + [\mathbf{v}]^\top \nabla \phi \right) - [\nabla]^\top \mathbf{D}^T \nabla \phi - Q^T = 0 \quad \text{in} \quad \Omega \tag{1}$$

with Dirichlet and Neumann boundary conditions:

$$\phi = \bar{\phi}(x, y, x, t) \quad \text{on} \quad \Gamma_\phi \tag{2}$$

$$q_n^T = \bar{q}_n^T(x, y, z, t) \quad \text{on} \quad \Gamma_q \tag{3}$$

where ϕ is the nodal variable (temperature $[^oC]$), ρ and c are the density $[kg/m^3]$ and the thermal capacity $[J/(kg\ ^oC)]$ of the material, $Q^{(T)}$ is a thermal source term, $\mathbf{v}$ is the average fluid velocity field (e.g. Darcy's velocity of the fluid transporting heat), q_n^T is the flow normal to the boundary, $\mathbf{D}^T$ is the constitutive matrix of the conduction problem $[J/(s\ m\ ^oC)]$, which is a diagonal matrix if the material is thermally isotropic, ∇ is the gradient operator vector $\nabla = \left[\frac{\partial}{\partial x}\ \frac{\partial}{\partial y}\ \frac{\partial}{\partial z}\right]$, and $[\ ]^\top$ denotes the transposed of a vector or a matrix (not to be confused with super index *T* which stands for "thermal").

1.2 FEM standard formulation for the advection problem

Performing the spatial discretization of Eq. (1) in the context of the Finite Element Method (FEM), applying the Divergence Theorem to the first term of the equation, applying the Galerkin weighing ($w = N^{(1)}, N^{(2)}, ...$) and performing the time discretization using the Finite Difference Method (FDM), the following algebraic system of equations is obtained:

$$\left[\frac{1}{\Delta t} \mathbf{C} + \theta\ (\mathbf{K} + \mathbf{K_c}) \right] \Delta \boldsymbol{\phi}_{n+1} = -(\mathbf{K} + \mathbf{K_c}) \boldsymbol{\phi}_n + \mathbf{f} \tag{4}$$

where $\boldsymbol{\phi}$ is the nodal temperature vector, $\mathbf{C}$ is the thermal capacity matrix, $\mathbf{K}$ is the thermal conduction matrix, $\mathbf{K_c}$ is the thermal advective matrix and $\mathbf{f}$ is the thermal force vector, which are obtained by the assembly of the contribution of each element of the mesh and are defined by:

$$\mathbf{C} = \int_\Omega \rho c\ [\mathbf{N}]^\top \mathbf{N}\ \mathrm{d}\Omega \tag{5}$$

$$\mathbf{K} = \int_\Omega [\nabla \mathbf{N}]^\top \mathbf{D}^T \nabla \mathbf{N}\ \mathrm{d}\Omega \tag{6}$$

$$\mathbf{K_c} = \int_\Omega \rho c\ [\nabla \mathbf{N}]^\top \mathbf{v}\, \mathbf{B}\ \mathrm{d}\Omega \tag{7}$$

$$\mathbf{f} = \int_\Omega [\mathbf{N}]^\top Q^T\ d\Omega - \int_{\Gamma_q} [\nabla \mathbf{N}]^\top \bar{\mathbf{q}}^T\ \mathrm{d}\Gamma \tag{8}$$

1.3 Large advection: Péclet number and numerical instabilities

It is well known [1] that the standard Galerkin weighting in FEM is very well suited for diffusion-dominated problems, but it performs badly when transport effects dominate over the conduction (large advection). Determination of whether the fluid velocities are high or low is generally based on the so-called Péclet number [3], a non-dimensional number that relates the velocity of advection and the rate of diffusion, and it is defined for thermal problems as:

$$Pe = \rho c \frac{v\, h_{car}}{2k^T} \tag{9}$$

where v is the average fluid velocity value in the porous medium (i.e Darcy velocity), h_{car} is the characteristic length of the element (length of the element in the direction of the flow) and k^T is the thermal conduction of the material.

A simple academic example in 1-D is presented in order to demonstrate that the standard Galerkin weighting leads to oscillatory results when $Pe > 1$. The geometry (Figure 1) consists of a horizontal rod element divided in 8 segments of equal length L. Boundary conditions are: prescribed temperature to 0ºC at the left-hand side node of the rod, prescribed temperature to 80ºC at the right-hand side node of the rod, and a constant velocity from left to right. With the only variation of the velocity magnitude, four results are obtained with different Péclet numbers (Figure 2), where it is observed that the solutions exhibit oscillations when $Pe > 1$. Thus, when the fluid velocities are high enough and the advection dominates the problem it is necessary to use a more appropriate numerical method that does not result in oscillatory solutions.

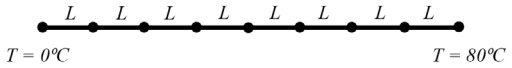

Figure 1: Geometry of the domain and boundary conditions.

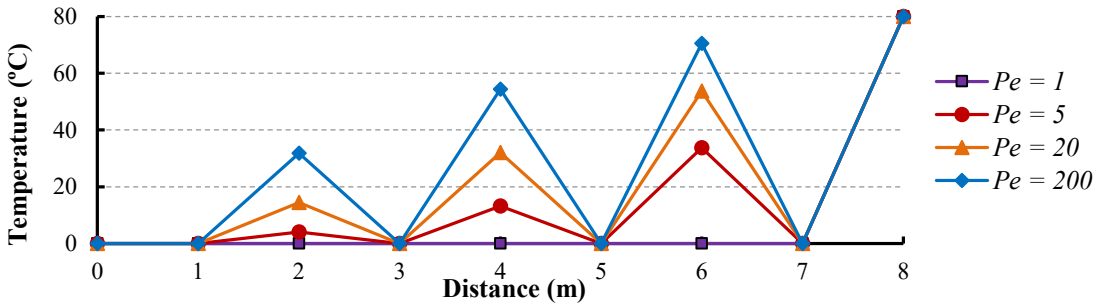

Figure 2: Solutions of the simple academic example for different velocities using the traditional Galerkin weighting method in FEM. Oscillations appears when $Pe > 1$.

2 STEADY-STATE LARGE ADVECTION USING THE SUPG METHOD

The most common method used in order to stabilize the diffusion-advection steady-state problem is the *Streamline Upwind Petrov-Galerkin* (SUPG) method [1]. The first *upwind* approach was proposed and applied in 1976 [4,5,6]. Then a new weighting function was proposed leading to the *Streamline Upwind* (SU) method [7], further developed as the SUPG method [8]. This method is based on the modification of the stiffness matrix by using modified weighting functions ($w \neq N^{(1)}, N^{(2)}, ...$), that are defined (in indicial notation) as:

$$w = N^{(a)} + \frac{\alpha_{opt}\, h_{car}}{2} \frac{v_i}{|\mathbf{v}|} \frac{\partial N^{(a)}}{\partial x_i} \tag{10}$$

where α_{opt} is the optimal value of α that must be used in order to obtain exact nodal values for any Péclet value [1]:

$$\alpha_{opt} = \coth|Pe| - \frac{1}{|Pe|} \tag{11}$$

Performing the spatial discretization of Eq. (1) by using the FEM, applying the Divergence Theorem to the first term of the equation and applying the Petrov-Galerkin weighing defined by Eq. (10), the following system of equations is obtained:

$$(\mathbf{K} + \mathbf{K_c} + \mathbf{K_{SUPG}})\,\boldsymbol{\phi} = (\mathbf{f} + \mathbf{f_{SUPG}}) \tag{12}$$

where $\mathbf{K_{SUPG}}$ and $\mathbf{f_{SUPG}}$ are the thermal stabilization matrix and the thermal force stabilization vector from the SUPG method. These matrices and vectors are obtained by the assembly of the contribution of each element of the mesh and are defined by:

$$\mathbf{K} = \int_{\Omega} [\mathbf{B}]^{\top}\, \mathbf{D}^{T}\, \mathbf{B}\, d\Omega \tag{13}$$

$$\mathbf{K_c} = \int_{\Omega} \rho c\, \mathbf{N}\, [\mathbf{v}]^{\top}\, \mathbf{B}\, d\Omega \tag{14}$$

$$\mathbf{K_{SUPG}} = \int_{\Omega} \left[\rho c \left(\frac{\alpha_{opt}\, h_{car}}{2|\mathbf{v}|}\, [\mathbf{v}]^{\top}\, \mathbf{B} \right) [\mathbf{v}]^{\top}\, \mathbf{B} + \left(\frac{\alpha_{opt}\, h_{car}}{2|\mathbf{v}|}\, [\mathbf{v}]^{\top}\, \boldsymbol{\nabla}\mathbf{B} \right) \mathbf{D}^{T}\, \mathbf{B} \right] d\Omega \tag{15}$$

$$\mathbf{f} = \int_{\Omega} [\mathbf{N}]^{\top}\, Q^{T}\, d\Omega - \int_{\Gamma_q} \mathbf{N}\, \bar{\mathbf{q}}^{T}\, d\Gamma \tag{16}$$

$$\mathbf{f_{SUPG}} = \int_{\Omega} \left[\left(\frac{\alpha_{opt}\, h_{car}}{2|\mathbf{v}|}\, [\mathbf{v}]^{\top}\, \mathbf{B} \right) Q^{T} \right] d\Omega \tag{17}$$

where $\mathbf{B} = \boldsymbol{\nabla}\mathbf{N}$ is the matrix containing the first-order derivatives of the shape functions. It must to be noted that the SUPG method is only applicable to steady-state regime.

2.1 Simple academic example: continuum medium in 2-D using the SUPG method

In order to verify that the SUPG method provides stable solutions when $Pe > 1$, a simple 2-D verification example is presented. The geometry consists of three horizontal layers of two different continuum materials (Figure 3 left). A constant flow velocity field from left to right (Figure 3 left) is imposed in the intermediate layer of the domain. The initial state of the thermal problem is shown in Figure 3 (right) and consists of a linear distribution of temperatures from left to right of the domain. The parameters for the numerical analysis are: heat capacity $\rho c = 1 \cdot 10^{-3}\, J/(m^3\, ^{o}C)$ and thermal conductivity $k^T = 2.5 \cdot 10^{-4}\, J/(s\, m\, ^{o}C)$.

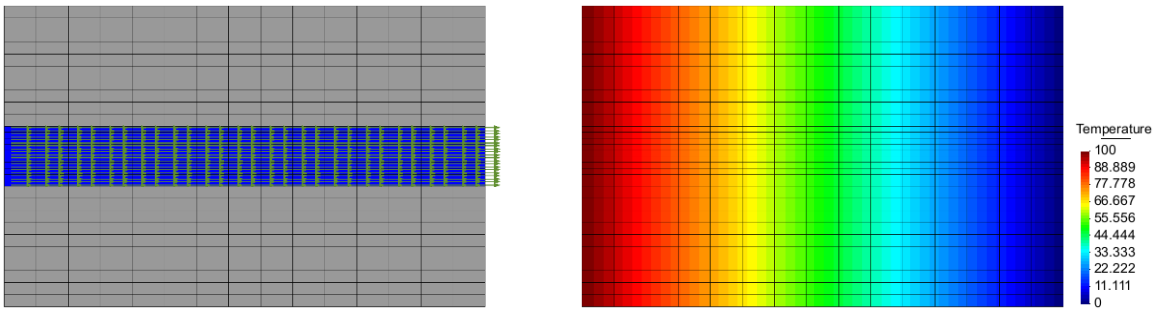

Figure 3: (left) Imposed velocities in the intermediate layer and (right) initial temperature distribution at *t=0* (after velocity application).

In the first calculations (Figure 4), the standard Galerkin weighting is used for a small advection problem, with Péclet numbers of 0.3 ($v = 0.006m/s$) in the left diagram, and 0.9 ($v = 0.017m/s$) in the right diagram. In both cases the SUPG and the standard FEM method both lead to the same stable solution depicted in the figure. Finally, the calculations are repeated using higher fluid velocities corresponding to $Pe = 7.2$ ($v = 0.135m/s$). In that case, Figure 5 (left) shows that the solution becomes oscillatory using the standard Galerkin weighting. However, using the SUPG method, the solution is stabilized (Figure 5 right).

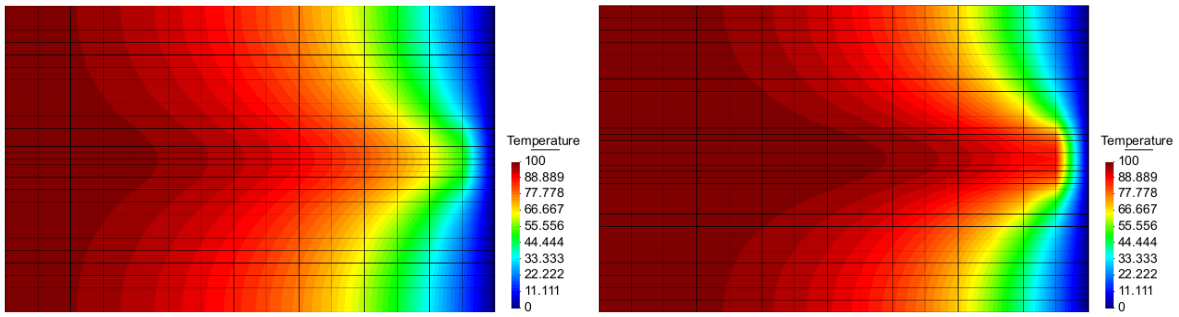

Figure 4: (left) Temperature distribution due to the applied velocities and *Pe = 0.3*. (right) Temperature distribution due to the applied velocities when the Péclet number increases but *Pe < 1* (*Pe = 0.9*).

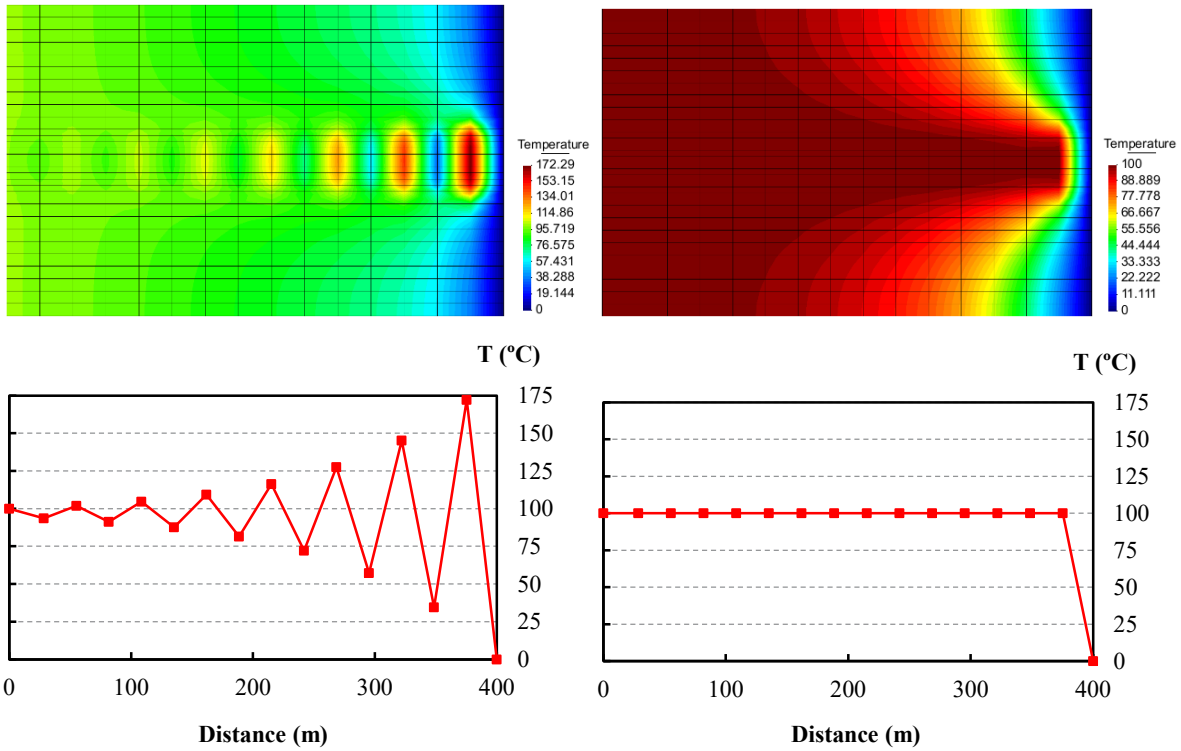

Figure 5: (left) Oscillatory distribution of temperatures using the standard Galerkin weighting when *Pe = 7.2* in the intermediate layer (the rest of the domain *Pe = 0*). (Right) Correct distribution of temperatures using the SUPG method for the same problem. Lower graphs represent the temperature distributions along the horizontal symmetry axis of the figures.

3 STEADY-STATE HEAT TRANSFER PROBLEM WITH LARGE ADVECTION FOR ZERO-THICKNESS INTERFACE ELEMENTS IN 2-D

In a 2D continuum, fractures and discontinuities may be represented individually by using double-nodded zero-thickness interface elements [9]. In this type of elements, one of the dimensions is collapsed to become 1-D line elements of "zero-thickness", and the integration is consequently reduced also by one order. The formulation of zero-thickness interface elements is composed of two parts (Figure 6): the formulation of the longitudinal flow along the interface and the formulation of the transversal flow across the interface, as described by [10,11]. The longitudinal flow is formulated along the mid-plane of the interface, and the nodal temperatures of the element are obtained by assuming that the temperature at each mid-plane node is the average of the temperature of the two nodes of the corresponding pair of the interface. Additional to the longitudinal flow, the existence of a discontinuity may also represent a resistance to the temperature flow in the transversal direction, which would result in a localized temperature drop across the interface. It is important to note that the large advection affects only the longitudinal flow. More details of the variables and geometry aspects that involve the double-nodded zero-thickness interface elements formulation can be found in [10,11,12].

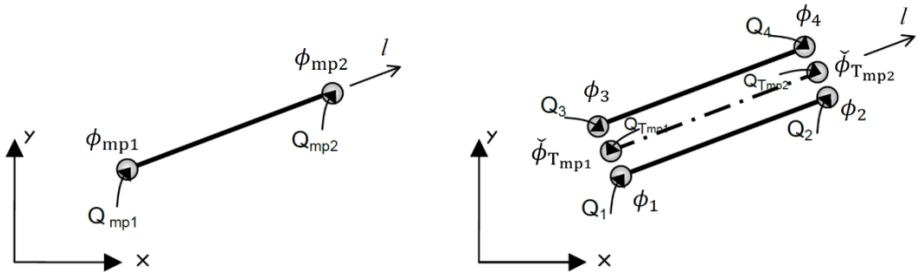

Figure 6: Zero-thickness elements used in the FE formulation with regard to longitudinal flow (left) and transversal flow (right).

3.1 Longitudinal flow

The longitudinal heat flow intensity q_{L}^{T} along the mid-plane of a discontinuity, corresponding to the accumulation of conduction (Fick´s law) plus advection flows in the transient regime, may be written as:

$$q_{\mathrm{L}}^{T} = -k_{\mathrm{L}}^{T} \frac{\partial \phi}{\partial l} + \rho c \phi v_{\mathrm{L}} \tag{18}$$

where k_{L}^{T} is the longitudinal thermal conductivity coefficient and v_{L} is the longitudinal velocity at the mid-plane of the interface element. The above q_{L}^{T} has the meaning of heat flow per unit area; by multiplying it by the interface aperture, r_N, one obtains the total heat flowing along the discontinuity (in 2-D per unit "depth" in the out-of-plane direction):

$$Q_{\mathrm{L}}^{T} = r_N \, q_{\mathrm{L}}^{T} = -r_N k_L^{T} \frac{\partial \phi}{\partial l} + r_N \rho c \phi v_{\mathrm{L}} \tag{19}$$

By enforcing heat conservation in a differential section of the interface element mid-plane (Figure 7), the continuity equation is obtained:

$$-\frac{\partial Q_{\mathrm{L}}^{T}}{\partial l} = r_N \rho c \frac{\partial \phi}{\partial t} \tag{20}$$

where source terms have not been considered for simplicity.

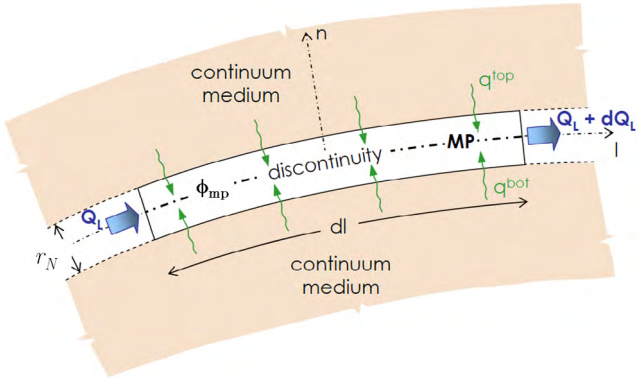

Figure 7: Thermal flow through a differential interface element.

Substituting now (19) into (20), leaving out transient terms, and taking into account that underlying flow is incompressible, leads to:

$$r_N \rho c \left(v_{\mathrm{L}} \frac{\partial \phi}{\partial l}\right) - r_N \frac{\partial}{\partial l}\left(k_L^T \frac{\partial \phi}{\partial l}\right) = 0 \quad \text{in} \quad \Omega_J \tag{21}$$

where Ω_J denotes the interface mid-plane domain. The boundary conditions are described by equations analogous to (2) and (3).

In order to stabilize the numerical solution of the steady-state large advection problem, the SUPG method defined in the previous section is used for zero-thickness interface elements.

Performing the spatial discretization of Eq. (21) along of the mid-plane of the interface by using the FEM, applying the Divergence Theorem to the first term of the equation, applying the Petrov-Galerkin weighing defined by Eq. (12), the following expression for the longitudinal flow along the mid-plane is obtained:

$$\mathbf{Q}_{\mathrm{L_{mp}}} = \left(\mathbf{K}_{\mathrm{L_{mp}}} + \mathbf{K}_{\mathbf{c},\mathrm{L_{mp}}} + \mathbf{K}_{\mathrm{L_{mp}}}^{\mathrm{SUPG}}\right) \boldsymbol{\phi}_{\mathrm{mp}} \tag{22}$$

where

$$\mathbf{K}_{\mathrm{L_{mp}}} = r_N \int_{\Omega_J} \left([\mathbf{B}_J]^{\mathrm{T}}\, k_L^T\, \mathbf{B}_J\right) \mathrm{d}\Omega_J \tag{23}$$

$$\mathbf{K}_{\mathbf{c},\mathrm{L_{mp}}} = r_N \rho c \int_{\Omega_J} \mathbf{N}_J\, v_{\mathrm{L}}\, \mathbf{B}_J\, \mathrm{d}\Omega_J \tag{24}$$

$$\mathbf{K}_{\mathrm{L_{mp}}}^{\mathrm{SUPG}} = r_N \rho c \int_{\Omega_J} \left(\frac{\alpha_{opt} h_{car}}{2|v_{\mathrm{L}}|} v_{\mathrm{L}} \mathbf{B}_J\right) v_{\mathrm{L}} \mathbf{B}_J\, \mathrm{d}\Omega_J + r_N \int_{\Omega_J} \left(\frac{\alpha_{opt} h_{car}}{2|v_{\mathrm{L}}|} v_{\mathrm{L}} \boldsymbol{\nabla}_J \mathbf{B}_J\right) k_L^T\, \mathbf{B}_J\, \mathrm{d}\Omega_J \tag{25}$$

$$\mathbf{B}_J = \frac{\partial \mathbf{N}_J}{\partial l} \qquad \boldsymbol{\phi}_{\mathrm{mp}} = \left[\phi_{mp}^{(1)}\ \phi_{mp}^{(2)}\right]^{\mathrm{T}} \tag{26}$$

In order to obtain the final FEM formulation related to the nodes of the mesh (and not to the mid-plane nodes), it is assumed that the temperature at the mid-plane is the average of the

temperature at the corresponding nodes of the element. Thus, the mid-plane temperatures of two-dimensional interfaces can be written in terms of the element's nodal temperatures (Figure 6) as:

$$\boldsymbol{\phi}_{\mathrm{mp}} = \begin{bmatrix} \phi_{mp}^{(1)} \\ \phi_{mp}^{(2)} \end{bmatrix} = \begin{bmatrix} \dfrac{\phi^{(1)} + \phi^{(3)}}{2} \\ \dfrac{\phi^{(2)} + \phi^{(4)}}{2} \end{bmatrix} = \begin{bmatrix} \frac{1}{2} & \frac{1}{2} \end{bmatrix} \boldsymbol{\phi}_{\mathrm{e}} = \widetilde{\mathbb{T}}_{\mathrm{L}}\, \boldsymbol{\phi}_{\mathrm{e}} \tag{27}$$

where $\widetilde{\mathbb{T}}_{\mathrm{L}} = \begin{bmatrix} \frac{1}{2} & \frac{1}{2} \end{bmatrix}$ is the longitudinal transference matrix and $\boldsymbol{\phi}_{\mathrm{e}}$ is the element temperature vector defined by:

$$\boldsymbol{\phi}_{\mathrm{e}} = \begin{bmatrix} \phi^{(1)} & \phi^{(3)} & \phi^{(2)} & \phi^{(4)} \end{bmatrix}^{\mathrm{T}} \tag{28}$$

Additionally, using the Principle of Virtual Work (PVW) in a discrete form leads to:

$$[\delta\boldsymbol{\phi}_{\mathrm{e}}]^{\mathrm{T}}\, \mathbf{Q}_{\mathrm{L_e}} = \left[\delta\boldsymbol{\phi}_{\mathrm{mp}}\right]^{\mathrm{T}}\, \mathbf{Q}_{\mathrm{L_{mp}}} \tag{29}$$

$$\mathbf{Q}_{\mathrm{L_e}} = \left[\widetilde{\mathbb{T}}_{\mathrm{L}}\right]^{\mathrm{T}} \mathbf{Q}_{\mathrm{L_{mp}}} \tag{30}$$

All the matrices and vectors defined at the mid-plane of the interface have to be transformed using the transference matrix, in order to obtain the similar relations between full element vectors including the pairs of nodes that appear in the FEM mesh. Substituting Eqs. (27) and (30) into Eq. (22) those relations are obtained as follows:

$$\mathbf{Q}_{\mathrm{L_e}} = \left(\mathbf{K}_{\mathrm{L_e}} + \mathbf{K}_{\mathbf{c},\mathrm{L_e}} + \mathbf{K}_{\mathrm{L_e}}^{\mathrm{SUPG}}\right) \boldsymbol{\phi}_{\mathrm{e}} \tag{31}$$

where

$$\mathbf{K}_{\mathrm{L_e}} + \mathbf{K}_{\mathbf{c},\mathrm{L_e}} + \mathbf{K}_{\mathrm{L_e}}^{\mathrm{SUPG}} = \left[\widetilde{\mathbb{T}}_{\mathrm{L}}\right]^{\mathrm{T}} \left(\mathbf{K}_{\mathrm{L_{mp}}} + \mathbf{K}_{\mathbf{c},\mathrm{L_{mp}}} + \mathbf{K}_{\mathrm{L_{mp}}}^{\mathrm{SUPG}}\right) \widetilde{\mathbb{T}}_{\mathrm{L}} \tag{32}$$

3.2 Transversal flow

Additional to the longitudinal flow, the existence of a discontinuity may also represent a resistance to the temperature flow in the transversal direction, which would result in a localized temperature drop across the interface (Figure 8). It is assumed that this temperature drop $\check{\phi}_N$ is related to the transverse heat flow q_N^T by a simple discrete version of Fick's law, in which the temperature drop plays the role of the temperature gradient:

$$q_N^T = \check{k}_N^T\, \check{\phi}_N \tag{33}$$

where $\check{k}_N^T$ is the transversal thermal conductivity of the interface.

The mid-plane potential thermal drop across the discontinuity is defined by the temperature difference between the two sides of the interface (Figure 8) as follows:

$$\check{\phi}_N = \phi_{bot} - \phi_{top} \tag{34}$$

$$\check{\boldsymbol{\phi}}_{\mathrm{N_{mp}}} = \begin{bmatrix} \check{\phi}_{N_{mp}}^{(1)} \\ \check{\phi}_{N_{mp}}^{(2)} \end{bmatrix} = \begin{bmatrix} \phi^{(1)} - \phi^{(3)} \\ \phi^{(2)} - \phi^{(4)} \end{bmatrix} = \begin{bmatrix} 1 & -1 \end{bmatrix} \boldsymbol{\phi}_{\mathrm{e}} = \widetilde{\mathbb{T}}_{\mathrm{N}}\, \boldsymbol{\phi}_{\mathrm{e}} \tag{35}$$

where $\widetilde{\mathbb{T}}_{\mathrm{N}} = [1 \quad -1]$ is the transference transversal matrix. That means that the potential thermal drop at the mid-plane node is the difference of potential between the two actual nodes.

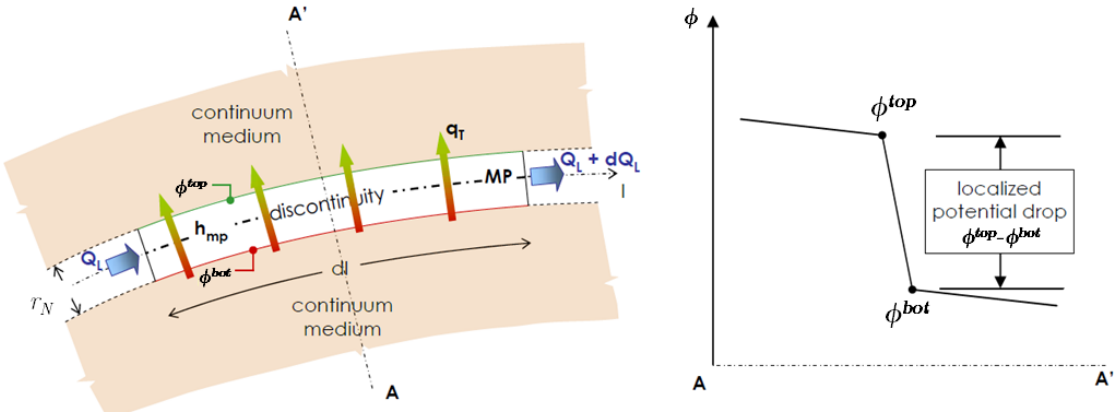

Figure 8: Scheme of the potential thermal drop across a differential interface element.

The FEM formulation for the mid-plane is obtained using the Principle of Virtual Work, which can be expressed for the transverse thermal flow problem as:

$$\left[\delta\check{\boldsymbol{\Phi}}_{\mathrm{Nmp}}\right]^{\mathrm{T}} \mathbf{Q}_{\mathrm{Nmp}} = \int_{\Omega_J} \delta\check{\phi}_{\mathrm{Nmp}}\, q^{T}_{N\mathrm{mp}}\, \mathrm{d}\Omega_J \qquad \forall\delta\check{\boldsymbol{\Phi}}_{\mathrm{Nmp}} \tag{36}$$

And substituting Eq. (33) into (36),

$$\mathbf{Q}_{\mathrm{Nmp}} = \mathbf{K}_{\mathrm{Nmp}}\check{\boldsymbol{\Phi}}_{\mathrm{Nmp}} \tag{37}$$

$$\mathbf{K}_{\mathrm{Nmp}} = \int_{\Omega_J} \left[\mathbf{N}_J\right]^{\mathrm{T}} \check{k}^{T}_{N}\, \mathbf{N}_J\, \mathrm{d}\Omega_J \tag{38}$$

where $\mathbf{K}_{\mathrm{Nmp}}$ is the transversal thermal conductivity matrix at the mid-plane. The vector of temperatures is defined by the same equation as in the longitudinal flow, Eq. (26).

Operating analogously to the longitudinal problem, the transversal thermal conductivity matrix at the nodes of the element is obtained:

$$\mathbf{K}_{\mathrm{N_e}} = \left[\widetilde{\mathbb{T}}_{\mathrm{N}}\right]^{\mathrm{T}} \mathbf{K}_{\mathrm{Nmp}}\, \widetilde{\mathbb{T}}_{\mathrm{N}} \tag{39}$$

3.3 Integrated formulation: longitudinal and transversal flow

To obtain an integrated conductivity matrix it is necessary to combine the longitudinal and the transversal flow as a sum of both, obtaining the final algebraic system of equation for each element as follows:

$$\left(\mathbf{K}_{\mathrm{L_e}} + \mathbf{K}_{\mathbf{c},\mathrm{L_e}} + \mathbf{K}^{\mathrm{SUPG}}_{\mathrm{L_e}} + \mathbf{K}_{\mathrm{N_e}}\right)\boldsymbol{\phi}_{\mathrm{e}} = 0 \tag{40}$$

where $\mathbf{K}_{\mathrm{L_e}}$, $\mathbf{K}_{\mathbf{c},\mathrm{L_e}}$, $\mathbf{K}^{\mathrm{SUPG}}_{\mathrm{L_e}}$ and $\mathbf{K}_{\mathrm{N_e}}$ are the longitudinal and transversal thermal conduction-advection matrices of the element defined by:

$$\mathbf{K}_{\mathrm{L_e}} = \left[\widetilde{\mathbb{T}}_{\mathrm{L}}\right]^{\top}\left(r_N \int_{\Omega_J}\left(\left[\mathbf{B}_J\right]^{\top} k_L^T\, \mathbf{B}_J\right) \mathrm{d}\Omega_J\right)\widetilde{\mathbb{T}}_{\mathrm{L}} \tag{41}$$

$$\mathbf{K}_{\mathbf{c},\mathrm{Le}} = \left[\widetilde{\mathbb{T}}_{\mathrm{L}}\right]^{\top}\left(r_N \rho c \int_{\Omega_J} \mathbf{N}_J\, v_{\mathrm{L}}\, \mathbf{B}_J\, \mathrm{d}\Omega_J\right)\widetilde{\mathbb{T}}_{\mathrm{L}} \tag{42}$$

$$\mathbf{K}_{\mathrm{Le}}^{\mathrm{SUPG}} = \left[\widetilde{\mathbb{T}}_{\mathrm{L}}\right]^{\top}\left(r_N \rho c \int_{\Omega_J}\left(\frac{\alpha_{opt} h_{car}}{2|\mathbf{v}_{\mathrm{L}}|} v_{\mathrm{L}} \mathbf{B}_J\right)\left[\mathbf{v}_{\mathrm{L}}\right]^{\top}\mathbf{B}_J\, \mathrm{d}\Omega_J + r_N \int_{\Omega_J}\left(\frac{\alpha_{opt} h_{car}}{2|\mathbf{v}_{\mathrm{L}}|} v_{\mathrm{L}} \boldsymbol{\nabla}\mathbf{B}_J\right) k_L^T\, \mathbf{B}_J\, \mathrm{d}\Omega_J\right)\widetilde{\mathbb{T}}_{\mathrm{L}} \tag{43}$$

$$\mathbf{K}_{\mathrm{N_e}} = \left[\widetilde{\mathbb{T}}_{\mathrm{N}}\right]^{\top}\left(\int_{\Omega_J}\left[\mathbf{N}_J\right]^{\top} \check{k}_N^T\, \mathbf{N}_J\, \mathrm{d}\Omega_J\right)\widetilde{\mathbb{T}}_{\mathrm{N}} \tag{44}$$

Finally, the global matrices of the system of Eq. (40) are obtained by the assembly of the contribution of each element of the mesh.

3.4 Simple academic example: steady-state large advection thermal problem in 2-D for interfaces using the SUPG method

The objective of this example is to compare some numerical results obtained with the standard Galerkin FEM method and the SUPG method, and verify that the latter provides stable solutions when *Pe >1* in a 2-D simple example using interfaces.

The geometry of this example consists of three horizontal layers with an interface at the symmetry axis (Figure 9 left), composed of 600 continuum elements and 20 interface elements. In order to visualize the heat transport, a known and constant velocity field from left to right ($v_{\mathrm{L}} = 0.057 m/s$, Figure 9 left) is imposed along the discontinuity, as a preferential path through the continuum medium.

The initial state of the thermal problem is shown in Figure 9 (right) and consists in a linear distribution of temperatures from left to right of the domain.

The numerical parameters for the continuum media are $\rho c = 1 \cdot 10^{-3}\, J/(m^3\, {}^{o}C)$ and $k^T = 7 \cdot 10^{-4}\, J/(s\, m\, {}^{o}C)$, and for zero-thickness interfaces $\rho c = 5 \cdot 10^{1}\, J/(m^3\, {}^{o}C)$, $k_L^T = 1 \cdot 10^{1}\, J/(m\, {}^{o}C\, s)$ and $\check{k}_N^T = 1 \cdot 10^{-03}\, J/(m^2\, {}^{o}C\, s)$.

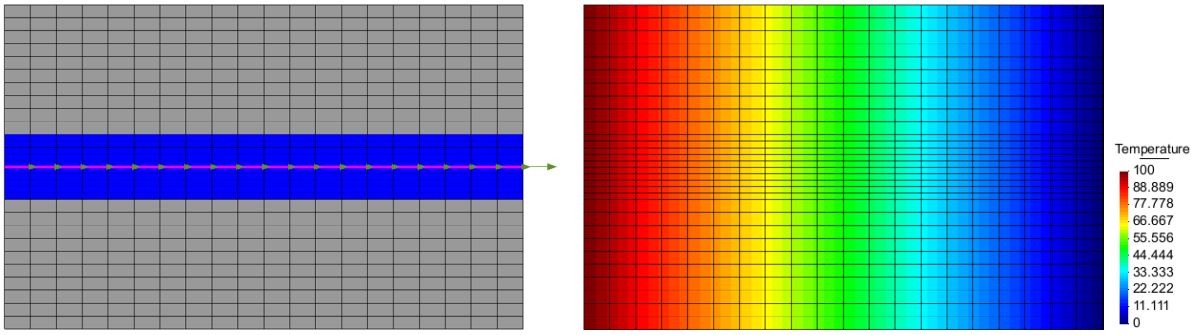

Figure 9: (left) Imposed velocities along the discontinuity (right) steady-state temperature distribution at t=0 (after velocity application).

In the first calculations, standard Galerkin weighing is used for the steady-state large advection problem (*Pe* = 3.8), leading to oscillatory results as shown in Figure 10 (left). However, using the new numerical solution (Petrov-Galerkin weighting, SUPG method) for

the interface element, the steady-state solution is stabilized, as shown in Figure 10 (right). In both cases the characteristic length of the element h_{car} is taken as the length of the element in the direction of the velocities.

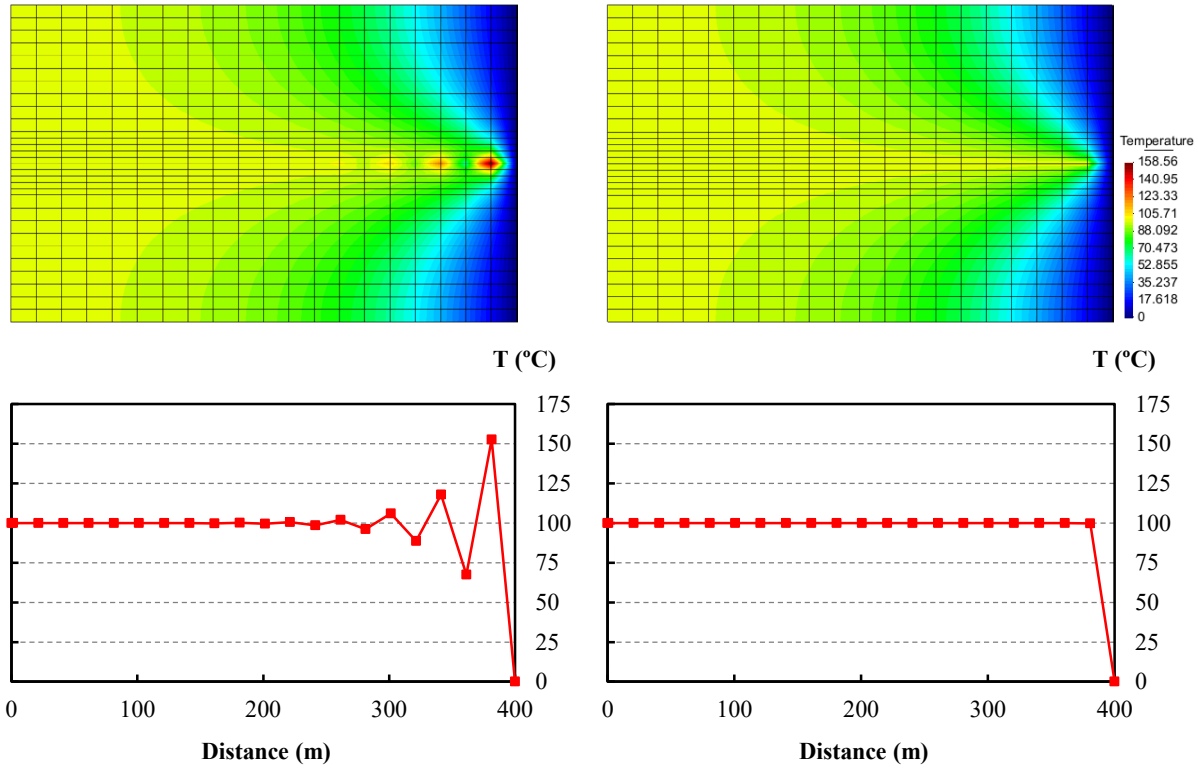

Figure 10: (left) Oscillatory distribution of temperatures using the standard Galerkin weighting when $Pe = 3.8$ along the discontinuity (the rest of the domain $Pe = 0$). (Right) Correct distribution of temperatures using SUPG method for the same problem. Lower graphs represent the temperature profiles along the mid-plane of discontinuity located in the symmetry axis of the problem.

4 CONCLUDING REMARKS

This paper describes the numerical FEM solution of the steady-state problem of heat flow in a porous medium, where a known Darcy velocity field of the pore fluid produces thermal transport with large advection. First, the traditional formulation using the standard Galerkin weighting has been reviewed. In this case a simple academic example shows that the solution becomes unstable when the advection dominates over the conduction ($Pe > 1$). Then, the SUPG method has been introduced, showing that this methodology stabilizes the solution when $Pe > 1$. Finally, the SUPG method has been formulated for 2-D zero-thickness interface elements. A verification example has been presented to show that this method is suitable for this type of elements when the advection is dominant for steady-state problems. Current work aims at the extension of the formulation presented to the transient problem with large advection, on the basis of the Taylor-characteristics method [1].

ACKNOWLEDGEMENTS
This work was partially supported by research grant BIA2016-76543-R from MEC (Madrid), which includes European FEDER funds, and 2017SGR-1153 from Generalitat de Catalunya (Barcelona). The first author also acknowledges his FPU scholarship from MEC (Madrid).

REFERENCES

[1] Zienkiewicz, O. & Taylor, R., *The Finite Element Method: Vol 3. Fluid Dynamics.* Fifth ed. Oxford: Butterworth-Heinemann (2000).
[2] Pérez, A. *THM coupling with large advection in fractured rock masses using zero-thickness interface elements.* Doct. Thesis. Universitat Politècnica de Catalunya, Barcelona (2018).
[3] Huysmans, M. & Dassargues, A. Review of the use of Péclet numbers to determine the relative importance of advection and diffusion in low permeability environments. *Hydrogeology Journal*. **13**:895-904, (2004).
[4] Zienkiewicz, O., Gallagher, R. & Hood, P., Newtonian and non-Newtonian viscous incompressible flow. Temperature induced flows and finite element solutions. *The Mathematics of Finite Element Methods (ed J. Whiteman). Academic Press, London.,* Volume II, (1976).
[5] Christie, I., Griffiths, A. & Zienkiewicz, O. Finite element methods for second orde differential equations with significant first derivatives. *International Journal for Numerical Methods in Engineering.* **10**:1389-96 (1976).
[6] Zienkiewicz, O., Heinrich, J. & Huyakorn, P. M. A., An upwind finite element scheme for two dimensional convective transport equations.. *Int. J. Num. Meth. Eng.,* **10**:131-144, (1977).
[7] Hughes, T. & Brooks, A. A multidimensional upwind scheme with no crosswind diffusion. *In ASME Monograph AMD-34 (Hughes, T.J.R., Ed.). NYC.,* Volume 34 (1979).
[8] Brooks, A. & Hughes, T. Streamline upwind/Petrov-Galerkin formulations for convection dominated flows with particular emphasis on the incompressible Navier-Stokes equations. *Computer Methods in Applied Mechanics and Engineering,* **32**:199-259, (1982).
[9] Goodman, R., Taylor, R. & Brekke, T.,. A model for the mechanics of jointed rock. *ASCE Journal of the Soil Mechanics and Foundations Division,* **94**:637–659, (1968).
[10] Segura, J., Carol, I. On zero-thickness interface elements for diffusion problems. *Int. J. Num. Anal.Meth.Geomech.,* **28**:947-962 (2004).
[11] Segura, J., Carol, I. Coupled H-M analysis using zero-thickness interface elements with double nodes. Part I: Theoretical model, and Part II: Verification and application. *Int. J. Num. Anal.Meth.Geomech.,* **32**:2083-2123 (2008).
[12] Garolera, D. *Zero-thickness interface elements in petroleum geomechanics: sand production and hydraulic fracture.* PhD Thesis. Universitat Politècnica de Catalunya, Barcelona (2017).